Integration of Solid Oxide Electrolyzer and Fischer Tropsch: a sustainable pathway for synthetic fuel

Giovanni Cinti[a], Arianna Baldinelli[a], Alessandro di Michele[b], Umberto Desideri[c*]

[a] Dipartimento di Ingegneria – Università degli Studi di Perugia, Perugia, Italy

[b] Dipartimento di Fisica e Geologia – Università degli Studi di Perugia, Perugia, Italy

[c] Dipartimento di Ingegneria dell'Energia, dei Sistemi, del Territorio e delle Costruzioni – Università degli Studi di Pisa, Pisa, Italy

* Corresponding author: Phone: +39 0502217375, email: umberto.desideri@unipi.it

Abstract

Because of their easy and widespread distribution and safe handling, liquid fuels are used in everyday life, to power vehicles, aircrafts, ships etc. The use of fuels from conventional fossil sources is now called for a more sustainable alternative. Hence, chemical energy storage of electricity generated by renewable sources into synthetic fuels represents an interesting solution, solving also other typical problems with renewables, such as grid stabilization.

In this framework, the present study deals with the production of synthetic green fuels by means of the Fischer Tropsch process, downstream a previous electricity-to-gas conversion achieved running a Solid Oxide Electrolyzer (SOE) stack in co-electrolysis. With regard to the state of the art, this study concerns the idea of integrating SOE and a Fischer Tropsch process in a small plant size, which is compatible with renewables power density. To this aim, fuel upgrading is supposed to be performed separately.

Based on experimental results on a Solid Oxide Cells stack operated in co-electrolysis, three system-level models were developed, evaluating the most performing option. Thus, considering a plant capacity of 1 bbl/day of liquid fuel, in the best scheme, the electricity-to-liquid efficiency was estimated to be 57.2%. Materials introduced to the system are simply water (33,701 ton/MJ) and carbon dioxide (79,795 ton/MJ). Whilst hydrogen is necessary to feed the SOE, net consumption is zero because it is recovered from Fischer Tropsch product lighter fraction.

Keywords: Solid Oxide Electrolyzer, Fischer Tropsch, gas to liquid, synthetic fuels, energy storage, distributed power plant

Introduction

High efficiency and use of renewable energy sources are two of the major keys for a sustainable development. Improving process efficiency requires a great technological effort, either to improve existing solutions or to look for brand-new concepts. The use of renewable energy sources, despite the significant deployment in the last years, still faces typical drawbacks such as the difficulty to predict the generated power exactly and to keep a stable power supply. Thus, in order to obtain the most out of unprogrammable energy sources (such as sun and wind), they have to be coupled with energy storage systems which separate the moments of supply and demand and mitigate electric grid stability issues. In addition to these points, environmental protocols call for a strict emissions control of greenhouse gases and other atmospheric pollutants.

In this paper, a system is studied that stores electricity by means of a high efficiency process, which produces a stable, high-density, safe and easy to handle energy vector. Among all the possible pathways to obtain a useful energy vector, the current work deals with chemical energy storage into a liquid fuel, which is preferable in many applications that cannot be operated with gaseous fuels. To this end, an efficient electricity storage is achieved by means of high temperature Solid Oxide Electrolyzers [1], which produce syngas out of water and carbon dioxide, operating in co-electrolysis. Carbon dioxide could be recovered from external processes, such as biogas or carbon capture from power plants' flue gases. Then, the electricity-to-gas process is followed by a gas-to-liquid conversion, by means of the Fischer Tropsch process. In this way the final utilization of synthetic carbonaceous fuels results in zero net carbon emissions. The use of solid oxide cells to electrolyze water was recently studied in several works dealing with high temperature steam electrolysis [2–11]; few literature results were found instead about CO_2 electrolysis [12–16]. The simultaneous electrolysis of CO_2 and H_2O (co-electrolysis), has been studied in the last years in a number of papers presenting experimental measurements [17–22] and system modeling.

Co-electrolysis offers several advantages: in spite of achieving separate steam electrolysis and the subsequent mixing with carbon dioxide in a dedicated reactor [23], a blend of hydrogen and carbon monoxide (referred as syngas) is obtained by simply operating an electrolyzer, without needing any additional component [1].

The produced syngas can be either directly used or further chemically processed (e.g. methanation, DME synthesis, Fischer Tropsch). The current technical, social and economic scenario is still requiring liquid fuels, favouring the synthesis of middle distillates (paraffinic hydrocarbons, mainly diesel and kerosene) [24]. For this reason, liquid fuel production via Fischer Tropsch synthesis represents a key-strategy to produce liquid fuels. From an historical point of view, this process is not new at all, since it was developed in Germany during the Second World War. At that time, the need for aircraft fuels pushed scientists to develop a method to gasify coal (which was locally available) into a valuable blend of liquid hydrocarbons. In such a manner, whilst oil-derived fuels were not accessible, liquid fuels could still be available. After the war, in some of the world coal richest areas the Fischer Tropsch technology allowed to produce liquid fuels: an example that is worth to mention is a Shell large refinery plant in South Africa. Similarly, where methane availability exceeds consumption, the Fischer Tropsch process was implemented downstream methane reforming.

Although large installations are normally used when using methane or coal as raw materials, many other technologies exist, which are suitable to produce a syngas to feed a Fischer Tropsch process [25]. As an example, biomass gasification is a possible primary step for a further gas-to-liquid process [26, 27]. Nevertheless, biomass-derived syngas could contain dangerous impurities and its composition is sensitive to environmental variables and feedstock heterogeneity. This is a clear disadvantage for a durable and correct operation of the catalysts used for the Fischer Tropsch synthesis. Conversely, the syngas composition from SOEs is controlled acting on the electrolyzer operational parameters; thus, the quality of the obtained syngas is improved and impurities affecting catalysts lifetime are absent. Moreover, with the aim of increasing the share of solar and wind power, the SOEs allows to use the soil more efficiently than producing biomass for energy utilization [28,29].

In several researches, evaluations of SOE-based systems were performed. In [30,31] a model considering the integration of SOEs with a nuclear plant was studied and a 52.6 % cycle efficiency was achieved. In [32], a thermodynamic study about the coupling of SOEs and a catalytic reactor for methane and DME synthesis was presented. Similarly, in [23], [24] SOE operation in an integrated system for the production of ethanol was simulated. The economic analysis of the system estimated a cost of 1.1 $ per kg of

ethanol synthetized. Finally, in [25] a model of an SOE-FT integrated system is presented where the main results are an overall efficiency of 51 % and liquid fuels final cost prediction of 4.4-15 $/GGE.

However, there are still several open issues to investigate: One of them is definitely the optimal plant size. While SOE technology can hardly be expected to be scale-up from the kW range up to the MW in a short time, FT synthesis is often associated with large installations in the order of 10,000 bbl/day, such as Sasol, Shell and PetroSA plants [5]–[7]. Alongside large-scale applications, many studies concerning smaller-size systems have begun in the recent years. Sunfire [23] is working on a Fischer Tropsch system to achieve a minimum liquid fuel production of 600 liters/day (4 bbl/day). Also Rentech [39] has been involved in a demo-installation with the productivity of 10 bbl/day. Finally, Velocys [40] patented a commercial 125 bbl/day modular reactor.

This study was based on the assumptions that the size of Fischer Tropsch processes can be reduced to have cost-effective applications also with smaller plant capacities, getting closer to what are foreseen SOE plant sizes. On one hand, Solid Oxide Electrolyzers can be made of several stack modules, achieving the required system capability. On the other hand, scaling down the Fischer Tropsch process, in order to integrate liquid fuels production into a RES-driven distributed energy generation system, is still a challenge. However, when considering a Fischer Tropsch process, two sections can be isolated: synthesis and refining. The first consists of transforming the incoming syngas into a syncrude blend made of liquid paraffins, alcohols and waxes, while the second is made of a series of expensive and size-sensitive processes, devoted to syncrude upgrading (E.g: hydrogenation and isomerization to achieve the proper Octane number). Considering the scenario of several distributed Fischer Tropsch facilities fed with gas coming from SOEs running on RES power, refining is not taken into account in this study and could still be conceived in a centralized plant receiving the syncrude blends from a number of smaller plants. Therefore, RES energy storage into a liquid medium does not include the upgrading of the primary syncrude to the refined products, which could be performed in a centralized plant, downstream many distributed facilities.

Coherently with such general approach, SOE and Fisher Tropsch units models were developed; the former is based on experimental data from an SOE stack, while the latter is based on assumptions derived from the literature. Three novel integration designs

were developed and studied, considering the overall system efficiency and other advantages, such as complexity reduction and integration with the surrounding environment.

Renewables-to-gas: Solid Oxide Electrolysers

In SOEs, electricity is fed to the system to drive electrochemical reactions whose products are valuable gases. Compared to a SOFC, the reactants are fed to the SOE cathode, which is the electrode, where reduction takes place, while the anode is the electrode where oxygen is obtained.

In the electrolysis process (Equation 1) water is split into hydrogen and oxygen, using heat and work as driving force. When carbon dioxide is also supplied with the reactants, co-electrolysis takes place. As it happens for water, carbon dioxide is reduced and it produces CO at the cathode and oxygen at the anode (Equation 2).

$$\boldsymbol{H_2O + 2e^- \rightarrow H_2 + O^{2-}} \quad \square H_0 = 241{,}57 \text{ kJ/mol} \qquad (1)$$

$$\boldsymbol{CO_2 + 2e^- \rightarrow CO + O^{2-}} \quad \square H_0 = 282{,}79 \text{ kJ/mol} \qquad (2)$$

ΔH is the energy necessary for the reactions and it is expressed as the well known sum of two contributions: Gibbs free energy and reaction entropy variation multiplied by the temperature (Equation 3). In fuel cells, the Gibbs free energy is the electrical work depending on the reversible potential between the cell electrodes (E_{rev}, Equation 4), Faraday constant (F) and electron mole flow associated to each mole of reactant (z; for example: one mole of water requires two moles of electrons as shown in Equation 1. Thus z=2).. Entropy has to be supplied in the form of heat, which makes SOE thermal losses internally valuable because they supply the electrolysis heat demand. When such irreversible thermal losses are equivalent to the heat demand, the energy balance is obtained and an energy equilibrium is reached that, for the aforesaid reasons, takes the name of thermoneutral. Thus, setting this as design operational point, all electrical input is transformed into hydrogen (or hydrogen plus carbon monoxide), i.e. into chemical potential energy, as defined in (Equation 4)

$$\boldsymbol{\Delta H = \Delta G + T\Delta S} \qquad (3)$$

$$\boldsymbol{\Delta G = z * F * E_{rev}} \qquad (4)$$

$$E_{tn} = \frac{\Delta H}{z \cdot F} = \mathrm{E}_{rev} + \frac{\mathrm{T}\Delta \mathrm{S}}{z \cdot F} \quad (5)$$

SOE efficiency (Equation 6) is calculated as the ratio between the chemical energy exiting the system, in terms of enthalpy ($\mathbf{\Delta H}$), and the electrical energy fed from the outside (E_e).

$$\eta = \frac{\Delta H}{\mathrm{E}_e} \quad (6)$$

Where E_e is the electrical energy input equal to current (z*F) multiplied the operating potential E.

Considering Equation 4 it can be easily calculated that efficiency is equal to 1 at thermoneutral conditions, where all electrical energy and relative heat losses are converted into chemical energy. In a real system, external thermal contribution may occur and thermoneutral voltage shifts towards higher or lower values if heat is respectively subtracted or supplied to the system.

Gas-to-liquid: Fischer Tropsch synthesis

Fischer Tropsch synthesis is a catalytic gas-to-liquid polymerization process, yielding light refinery gases, a crude blend of hydrocarbons (gasoline and diesel cuts) and waxes. The synthesis process typically takes place at temperatures in the range of 200-240°C (for low temperature FT applications – LTFT) and 300-350°C (high temperature FT applications – HTFT) and pressure of about 20-40 bar [41].

State-of-the-art reactors use two types of catalyst: iron and cobalt. The choice of the best option is led by the application. To this end, the latter is more selective towards middle carbon cuts, maximizing diesel production. In addition, other features that support the employment of cobalt catalysts are: better performances in terms of CO conversion rates and reduced ageing phenomena. Cost and a poor flexibility to H_2/CO ratio are main drawbacks. However, the second is not an issue whereas syngas composition can be regulated. Thus, a SOE unit assures a constant gas composition with a designed H_2/CO.

From the chemical point of view, Fischer Tropsch synthesis is a catalytic polymerization consisting of a multi-step mechanism. The first is CO adsorption onto

the catalyst surface. Hence, the kinetic of the process is mainly controlled by CO reaction rate [42]. After, adsorbed CO loses its oxygen atom and it establishes chemical bonds with hydrogen atoms, creating the basic monomer $-CH_2-$. The reaction mechanism carries on until the chain reaches termination and, then, molecules are desorbed. Typical products, hence, are hydrocarbons, alcohols, aldehydes, chetons and so on, all associated with a variable length $-CH_2-$ bone. The specific catalyst and the operative conditions (temperature and reactants partial pressure) govern the carbon chain growth, determining the process yield upon each carbon cut. Process chemistry is expressed by the following reactions, concerning paraffins (7), olefins (8) and alcohols (9) production. Varying the integer value attributed to *n*, Reactions 7-9 describe the stoichiometric reactions of all the possible Fischer Tropsch products, ranging from lower carbon cuts (n=1 methane, n=3 propane) up to upper ones (n>30, paraffinic waxes).

$$\mathbf{n\ CO + (2n + 1)H_2 \rightarrow C_nH_{2n+2} + n\ H_2O} \quad (7)$$

$$\mathbf{n\ CO + 2n\ H_2 \rightarrow C_nH_{2n} + n\ H_2O} \quad (8)$$

$$\mathbf{nCO + 2n\ H_2 \rightarrow C_nH_{2n+1}OH + (n-1)\ H_2O} \quad (9)$$

Typical Fischer Tropsch catalysts exhibit a variable selectivity upon different carbon cuts. This behaviour is described by chain growth probability factor, called α.

INSERT FIGURE 1 HERE

In Figure 1, a typical products distribution is depicted: the vertical axis reports the mass yield, while the horizontal axis the chain growth probability. Thus, carbon cuts are grouped according to the category listed in Figure 1 legend.

From the simple explanation of the mechanism provided previously, it is possible to argue that the closer is α to 1, the more compounds with high carbon number are likely to form. Cobalt catalysts exhibits α values in the range of 0.8-0.94: this is the reason why middle distillates are most favoured product of a Co-based Fischer Tropsch process (Figure 1).

Besides catalyst performance, even process conditions have an influence on selectivity, and consequently on the yield associated to each carbon cut. When temperature is increased, selectivity shifts products yield to lower carbon number and chain branching

is favoured. Alcohols synthesis is inhibited. Olefins-to-paraffins ratio, instead, does not change with temperature when dealing with cobalt catalysts. Else, the effect of increasing pressure is to shift the chain growth probability to higher carbon cuts and to disadvantage branching. Since the process is controlled by CO reaction rate, this determines the conversion efficiency. For SoA catalysts, 80%-90% conversion efficiency is expected.

Finally, it is also interesting to point out that Reactions 3-5 are globally exothermal. Hence, the perspective to integrate a Fischer Tropsch process in an system with heat sinks such as SOEs, is very challenging.

Experimental activity

To support SOE unit modelling, a preliminary experimental activity was performed on a Jülich four-cells short stack (Table 1). Cell materials and test bench equipment are deeply discussed in a previous study [43], concerning high temperature steam electrolysis by means of Solid Oxide cells.

INSERT TABLE 1 HERE

SOE stack is kept at constant temperature (750°C) in an electric furnace. Such temperature was selected because is a trade-off between efficiency (high temperature) and material resistance (lower temperature). 750°C is considered state of the art for SOFC materials and, consequently, also for SOE. Temperature variation is measured by two thermocouples placed on the interconnection plate inside the stack, the first close to the cathode inlet and the second close to the air inlet. Water is vaporized and mixed with pure gases by a Controlled Evaporation Mixture (CEM) system. Both inlet feed streams are heated up to 650 °C before entering the furnace.

INSERT TABLE 2 HERE

Table 2 reports operating conditions used in the experimental activity. Tests were carried out supplying the anode with a constant air flowrate and varying cathode inlet feedstream composition in terms of H_2O:CO_2:H_2. Hydrogen is introduced to keep a reducing atmosphere and to protect materials from oxidation. Two compositions were considered with different H_2O:CO_2:H_2 ratios: namely 30-60-10 and 40-50-10.

$$V(j) = OCV + ASR * j \quad (10)$$

INSERT FIGURE 2 HERE

Process Modelling

The paper aims at presenting the concept of electricity-to-liquid conversion accomplished by means of an integrated system consisting of a Solid Oxide Electrolyzer unit and a Fischer Tropsch reactor. The concept study was developed with a system-level model: in particular, three possible system layouts were studied, evaluating both efficiency and impacts in terms of water consumption and carbon dioxide stored. Else, SOE unit size is determined, in order to fulfil Fischer Tropsch syngas requirements for a designed tail-end productivity.

All the calculations have been performed by using the Aspen Plus® environment, and the Nist libraries.

The plant is divided in two main sections: the first one is the electrolyzer unit, the second the liquid fuel synthesis unit. While SOE is supposed to operate at environmental pressure, to favor middle distillates selectivity, Fischer Tropsch reactor is pressurized at 20 bar. Therefore, the two main sections need to be linked by a multistage intercooled compressor. In addition, heat recovery is performed at several levels of the process, so that reduced net heat demand contributes to increase the overall system efficiency.

Because of the down-scaling of the FT liquid fuel synthesis, crude refining is not provided, with the exception of a raw pre-flash separation that divides purge water from hydrocarbons and light refinery gases (hydrogen and carbon products with n<=4). Hence, crude fuel upgrading is to be done in a separate large scale optimized plant, where primary Fischer Tropsch products can be easily transported.

In the following, a detailed discussion is presented, describing how system parts were modeled. Afterwards, system performance evaluations of three different designs are shown.

SOE model

Since Aspen Plus® does not provide a built-in block to simulate the operation of a Solid Oxide Electrolyzer this component has been modeled merging basic Aspen Plus® blocks and customized Fortran® routines. This unit considers SOE inlet gas temperature at 120°C. The energy to increase reactants temperature from ambient conditions to 120°C, included water evaporation, are not taken into account in this

paragraph and are discussed in the system integration section. Therefore, the SOE model consists of three main blocks: cathode, electrolyte and anode.

Cathode is the reactants electrode, where inlet gases are supplied and electrolysis takes place. The Cathode was modelled by using a first equilibrium reactor, a splitter block, a stoichiometric reactor, a mixer block and, a second equilibrium reactor. The first equilibrium reactor adjusts the cathode feedstream composition considering the stack temperature and pressure, according to Reaction 6-7. The splitter block divides the reactants stream into two branches, according to the reactants utilization. Reactants utilization (U_{react}, Equation 11) represents the conversion rate of reactants involved in the electrochemical process (Equations 1-2). It is defined as the ratio between the current fed to the electrolyzer (j*A) and the maximum current needed to have all the reactants converted into products (z*F*$Q_{react,}$ where z is the number of electrons given by a mole of reactants, F is the Faraday constant and Q_{react} is the total reactant flowrate). U_{react} is assumed to be an input data for the model and it is set at 0.5.

$$\boldsymbol{U_{react} = \frac{j*A}{z*F*\dot{Q}_{react}}} \quad (11)$$

Then, the stoichiometric reactor is fed with the reactants flow corresponding to the superimposed reactants utilization rate. The stoichiometric reactor accomplishes water (1) and carbon dioxide (2) electrochemical reactions. Oxygen is removed from Co-electrolysis products and mixed together with the unreacted stream exiting from the upstream splitter in the following mixer block. Finally, an equilibrium reactor balances the products composition at the cathode outlet. The latter block takes into account the occurrence of RWGS (12) and methanation (13). All the reactions take place at atmospheric pressure and 750°C.

$$\mathbf{CO_2 + H_2 \rightarrow CO + H_2O} \quad (12)$$

$$\mathbf{CO + 3H_2 \rightarrow CH_4 + H_2O} \quad (13)$$

The electrolyte layer is modelled with a simple separator block, which separates oxygen anions (see Equations 1-2) from the other cathode products. In such a manner, oxygen is separated from syngas.

The anode is the air electrode. Its function is to extract oxygen from the stack. In the model it is simulated with a gas mixer, whose inlet feedstreams are oxygen from the electrolyte and sweep air. It is common practice to supply air to the anode side because it facilitates oxygen removal and it lowers cells overpotentials due to a high oxygen concentration. Anode-sweep air flowrate is set in order to get an oxygen partial pressure of 0.5 bar at the anode exhausts. Lowering oxygen partial pressure would cause an increase in the sweep-air flowrate required and, accordingly, a larger heat demand to keep the anode compartment temperature constant.

Finally, both anode and cathode feed streams temperature is increased to the expected value required at the inlet of the stack (650°C) by means of heat exchanger blocks. In detail, heat is regerenatively recovered both in the cathode and the anode to increase gas inlet temperature.. The amount of heat available is sufficient because oxygen stream from the electrolyte increases the total flow and, consequently, its thermal in comparison with the anode inlet.

Assuming to operate the SOE stack at thermoneutral conditions, cathode feedstream composition was controlled to produce a syngas featuring the optimal H2/CO ratio for the downstream Fischer Tropsch process. As it was explained before, when middle distillates (which end in diesel cuts) are the preferred products, cobalt catalysts exhibit an enhanced selectivity for this particular application, yet requiring very slight variations of reactants H2/CO ratio. Thus, to achieve an H2/CO=2.1 ratio at the stack outlet, cathode inlet composition is set according to the ratio H_2O:CO_2:H_2 58: 34.5:7.5, that is in within the reactants compositions used in the stack experimental characterization (Table 2). Moreover, hydrogen is fed to the cathode, in order to assure a reducing atmosphere at the reactants electrode; as a design specification for the model development, hydrogen concentration in the cathode feed has to be in the range 7-8% [43].

In order to simulate the electric behavior, a Fortran® subroutine was implemented in the model. Thermoneutral conditions (5) are deduced from the overall enthalpy variation occurring between the cathode inlet and the cathode outlet. Thus, ΔH (related to the thermoneutral potential according to Equation 5) is the sum of three terms: sensible heat necessary to bring cathode reactants up to the stack operational temperature (750°C) after recovering heat, co-electrolysis reactions enthalpy (cathode

stoichiometric reactor net duty) and equilibrium reactions enthalpy (equilibrium reactors net duty). Stack voltage is then set equal to thermoneutral voltage deduced from Equation 5. Hence, the operational point current density is calculated by means of the polarization curve, presented in the Experimental Section (10). Considering this routine, electric power consumed by the SOE stack is determined. Then, system energy balance will lead to the calculation of the right stack size as it is discussed at the end of this Section.

Fischer Tropsch process model

Electrolysis syngas is drawn at the SOE outlet and then sent to an auxiliary section made of an intercooled compressor to achieve the required pressure before entering the Fischer Tropsch reactor. Fischer Tropsch synthesis is assumed to take place at 20 bar and reactor is kept isothermal at 230°C [41].

The Aspen Plus® model of this part of the system is sketched with a splitter block, a stoichiometric reactor, a mixer block and a flash separator.

The splitter block divides the syngas feedstream in two: the first part enters the stoichiometric block and its flowrate fraction, with respect to the total dry syngas flowrate, is calculated from the expected CO conversion efficiency (ε_{CO}, Equation 14) [44]; the second part is shortcut to the mixer, where it is combined with Fischer Tropsch products exiting the stoichiometric reactor. In the model ε_{CO} is set to 0.87 [44]. Splitter block rates were regulated accordingly, with an iterative calculation.

$$\boldsymbol{\varepsilon_{CO} = 1 - \frac{x_{COout}}{x_{COin}}} \quad (14)$$

The stoichiometric reactor accomplishes several reactions (Table 3), providing the conversion of hydrogen and carbon monoxide to a hydrocarbon blend of alkanes and alkenes. Process selectivity towards each path is implemented in the block, using a mathematical model which considers the hydrocarbon chain growth probability over the possible products spectrum. The mathematical model employed is the Anderson-Schulz-Flory (ASF) distribution [4] described by Equation 15. For every carbon cut (represented by the parameter *n*), it relates the products mass fraction (*Wn*) to the catalyst chain growth probability ($\boldsymbol{\alpha}$).

$$\boldsymbol{W_n = n\alpha^{n-1}(1-\alpha)^2} \quad (15)$$

The ASF function does not take into account any difference among compounds containing the same number of carbon atoms. In other words, for a given n, that is representative of a particular carbon cut, *Wn* is then the sum of paraffins, oleifins, alcohols and minor species.

However, some distinctions within the same carbon cut can be done considering the catalyst features. In this work we assumed to work with cobalt catalysts; thus, the following approximations are acceptable:

- alcohols and other oxygenated and aromatic hydrocarbons synthesis are not favored, so all possible products derived from Equation 9 can be neglected;
- the relative amount of alkanes and alkenes can be modeled as well. Therefore, the olefins-to-paraffins ratio (O/P) is introduced in Equation 16. According to this model [46], for every carbon number n, O/P depends only on the catalyst nature, represented by the constant coefficient *k*. From the model assumptions, k is set to 0.3.

$$\left(\frac{O}{P}\right)_n = e^{-k\,n} \tag{16}$$

INSERT TABLE 3 HERE

For simplicity, the model considers just a discrete number of possible products, as it is summarized in Table 3: each carbon cut, corresponding to an n range, is represented by one or two model compounds.

Thus, assuming a chain growth probability $\alpha = 0.94$ [41], the ASF distribution in the model is evaluated for every integer n ranging from 1 up to 50. Then, considering Table 3 *n* ranges, the overall mass fraction yield is evaluated for every discrete *n* (implementing ASF mathematical model). In order to consider the olefins production per every carbon cut, the *O/P* ratio was calculated and applied to the discrete ASF distribution results. From those data the model provides the mass yield for every discrete cut.

Then, the stoichiometric reactor outlet stream and the dry syngas streams that bypassed the reactor are mixed in a mixer block, and gas phase equilibria are adjusted through Gibbs energy variation minimization.

At the end, resulting products (“syncrude”) are sent to a flash separator (condenser) that models the first stage of the raw products upgrading. Light gases, liquid phase (“crude”) and water are separated.

Flash separator temperature is calculated to optimize phase separation and minimize the solubility of hydrocarbon into water.

The model of the Fischer Tropsch section ends without considering further refining, for the reasons already described.

Auxiliaries

Between the SOE and FT sections some auxiliary components are necessary. In particular, there are a condenser and an intercooled compressor. The condenser is necessary because water needs to be removed from the Fischer Tropsch feedstream. Since the SOE operates at 50% reactants utilization, syngas still contains much water. Water condensation and removal is necessary for three reasons:

reducing compressor feedstream mass flowrate, compression work substantially decreases, with a benefit on system efficiency;

lowering compressor inlet stream temperature, compression work decreases;

when water content is high, Fischer Tropsch catalysts degradate, leading to a loss of efficiency.

Water separation is mandatory for the mentioned reasons; in addition to that, water separation from syngas allows water recycling, in order to reduce process net material consumption.

Therefore, water was condensed by means of a flash separator operating at ambient pressure and 35°C. Condenser temperature is determined according to the steam partial pressure in syngas collected at SOE outlet. Since steam fraction in syngas is expected to be around 30% at the given operational point of the electrolyzer, condenser temperature must be lower than 68°C. Afterwards, dry syngas is sent to a multistage intercooled compressor that achieves an overall pressure ratio of 20. In the model, this is simulated with two compressor blocks, separated by a heat exchanger. Syngas temperature of the heat exchanger outlet is controlled to have the gas exiting the last compressor stage at the temperature required by the Fischer Tropsch synthesis. Finally, other auxiliary components are introduced in the system, but their operation will be discussed in the following section because it concerns the specific layout that is implemented.

System configurations

In this study, three plant layouts were considered (Figure 3). In particular, they are referred as layout A, B and C. For all the layouts considered, system design specifications are Fischer Tropsch synthesis productivity (set to 1 bbl/day) and SOE cathode outlet stream quality, expressed as H_2/CO ratio (set to 2.1). Then, according to specific system layouts (A, B, C), SOE feeding flowrate and composition are determined accordingly. Hereinafter, a description of each layout is reported.

Layout A is the base case and it consists of an SOE section connected to the FT section through an intercooled compressor (Figure 3, A). Layout A features an open loop strategy and no material recirculation is performed. Consequently, SOE feeding flowrates (water, carbon dioxide and hydrogen) are calculated in order to provide enough dry syngas for the nominal FT productivity of 1 bbl/day.

Layout B and C have closed loops, performing material recirculation and heat recovery. This strategy aims at improving overall efficiency, while reducing net material consumptions. As far as material recycling is concerned, both waste water and light gases coming out from Fischer Tropsch synthesis can be re-used within the system itself, with a noticeable effect on the overall plant efficiency. Water is produced as a waste in two sections of the plant: syngas condenser prior intercooled compressor and syncrude condenser downstream the FT synthesis. Water recovered from syngas cooling has a fairly good purity because of the negligible solubility of the other gases. The only exception is carbon dioxide: however, low carbon dioxide traces are acceptable when recirculating recovered water to the SOE inlet. Water removed from the syncrude stream might contain hydrocarbons trace, which is not a problem, since they are supposed to be reformed. Then, light gases fractions extracted from the Fischer Tropsch syncrude exhibit high hydrogen and carbon dioxide concentrations. This makes those gases recirculation to the SOE inlet very attractive. Light gases contain lower hydrocarbons as well (propane and propene, according to the model proposed above (Table 3).

In layout B (Figure 3, B), syncrude light gases are sent to a reformer and, then, reformate gas enters a shift converter. Reformer and shift converter water requirements are fulfilled with recycled water. Then, the gas stream exiting the shift converter is recirculated to the SOE cathode inlet. Net SOE reactants demand is calculated to reach

the nominal flowrate required according to the plant size. Operating separately reforming and shift, temperature control allows reaching maximum conversion efficiency in both reformer and shift converter.

INSERT FIGURE 3 HERE

In the model, both reformer and shift converter are simulated with the Aspen Plus® equilibrium reactor. Reformer block operates at 700°C and 1 bar with a S/C=2, while shift conversion takes place at 310°C and 1 bar. Shift conversion temperature is much lower because typical reforming temperature will favor the reverse equilibrium, decreasing the final hydrogen concentration. Thus, a heat exchanger to perform gas cooling is necessary in between the two reactors. Finally, gas coming out of the shift converter is ready to be mixed with reactants makeup stream feeding the cathode fresh feed stream before the stack inlet. Overall SOE reactants stream pre-heating is assured by the mixing of the makeup stream and shift products. Despite this fact, the system complexity grows because of additional system units. External reforming and shift conversion make up a process that is globally endothermal, increasing the system heat demand. Then, to keep overall efficiency at a high level, heat recovery also requires a supplementary heat exchanger.

INSERT TABLE 4 HERE

Differently from layout B, layout C has no external reforming (Figure 3, C), although some streams are recirculated. In particular, Fischer Tropsch light gases and recovered water are directly recirculated to the SOE cathode inlet. Since SOE operational temperature is 750°C and SOE catalysts are nickel-based, methane and low hydrocarbon reforming is likely to happen inside the SOE. Shortcutting unreformed gases directly into the stack simplifies the plant scheme, reducing the components number. Nonetheless, cathode recycled streams are cooled down to water condensation temperature before being sent to the SOE inlet. This increases the heat demand to reach 120°C at the SOE inlet. Reforming and shift reaction happen at stack temperature, yielding a mixture of hydrogen, carbon dioxide and carbon monoxide. Yet, small amounts of higher hydrocarbons produced in the Fischer Tropsch reactor could be present in the gas phase coming out of the syncrude condenser. While a large steam concentration in the SOE feedstream favors hydrocarbons reforming, some hydrocarbon fractions could be responsible of carbon deposition on the SOE stack. In such

configuration, the necessary energy to support internal reforming is provided by the SOE stack; then, running the stack at its maximum efficiency, thermoneutral voltage is shifted with regard to the other layouts and there is also a change in the power density.
In this case, SOE cathode feedstream water fraction must fulfill both reforming and electrolysis demand (always keeping SOE reactants utilization at 50%). System layouts just discussed are compared considering both overall and single blocks performance. Regardless of the configuration, the Fischer Tropsch block efficiency and productivity is the same in any case, because operational and inlet conditions are fixed as design specifications. Therefore, A, B and C configurations show different efficiency at system level. Clearly, besides different stream recirculation strategies, also heat management changes, affecting the overall efficiency.
All design specifications are summarized in Table 4, reporting the model section whom they refer to and the system layout in which they are implemented.

Parameters definitions

Some definitions are needed to compare the different layouts investigated. All the definitions are based on the lower heating value. In detail, they are: SOE block efficiency in Equation 17 (it considers as inputs electrical power, thermal power and power associated to hydrogen, while output power is the term related to syngas exiting the stack) and FT block efficiency, related both to syncrude (18) and crude (19) production.

$$\eta_{SOE} = \frac{\sum_{syngas} \dot{m}_j * LHV_j}{V * i + Q_{net,SOE} + \sum_{soe} \dot{n}_i * LHV_i} \quad (17)$$

$$\eta_{FT} = \frac{\sum_{syncrude} \dot{m}_j * LHV_j}{\sum_{syngas} \dot{n}_i * LHV_i} \quad (18)$$

$$\eta_{GTL} = \frac{\sum_{crude} \dot{m}_j * LHV_j}{\sum_{syngas} \dot{n}_i * LHV_i} \quad (19)$$

While, the overall system performance is described by η_{tot} (Equation 20), dividing the crude stream enthalpy flow per system total power consumption (SOE feedings in terms of hydrogen, electricity and heat, compressors' work and total heat sinks requirements).

$$\eta_{tot} = \frac{\sum_{crude} \dot{m}_j * LHV_j}{\sum_{soec} \dot{n}_i * LHV_i + (VI)_{soec} + W_{aux} + Q_{net,system}} \quad (20)$$

Then, concerning the Second Law of Thermodynamic, other two parameters are introduced: the ratio between electrical input power and total input power (Equation 21) and the exergetic efficiency (Equation 22).

$$\frac{p_{el}}{p_{tot}} = \frac{(VI)_{soec}}{\sum_{soe} \dot{n}_i * LHV_i + (VI)_{soec} + W_{aux} + Q_{net,system}} \quad (21)$$

$$\eta_{ex} = \frac{\sum_{crude} \dot{m}_j * LHV_j}{\sum_{soe} \dot{n}_i * LHV_i + (VI)_{soe} + W_{aux} + \sum_k Q_k \left(1 - \frac{T_0}{T_k}\right)} \quad (22)$$

Finally, primary materials (hydrogen, water and carbon dioxide) consumptions are estimated, relating the net consumptions achieved to the system nominal power. Therefore, consumption factors are introduced in Equations 23 to 25.

$$H_2O_{consumption} \left[\frac{ton}{MJ}\right] = \frac{net\ water}{power\ out} \quad (23)$$

$$H_{2\ consumption} \left[\frac{ton}{MJ}\right] = \frac{net\ H2}{power\ out} \quad (24)$$

$$CO_{2\ consumption} \left[\frac{ton}{MJ}\right] = \frac{net\ CO2}{power\ out} \quad (25)$$

Stack sizing

In the Introduction section, the working principle of an SOE was explained, with particular attention to the thermoneutral voltage that achieves the highest SOE efficiency in any system configuration. Conversely, because of different system configurations implemented in layouts A, B and C, the enthalpy difference that determines the thermoneutral voltage changes. In particular, for layout A and B enthalpy differences take into account the electrochemical process occurring in the stack, SOE equilibria and sensible heat necessary to rise SOE cathode temperature (covering the thermal gap between 650°C and 750°C). Layout C enthalpy difference includes the enthalpy change caused by the reforming of light hydrocarbons recycled to the stack from the syncrude products separation. Owing to the endothermal contribution of reforming, the operational voltage at thermoneutral conditions in layout C is expected to be higher.

Moreover, since the components total flow is controlled by the final liquid fuel productivity, the SOE block has to supply a suitable amount of syngas to the Fischer Tropsch block.

As a consequence, it is necessary to calculate the stack size for every system layout. To this end, the model developed in this study permits to evaluate SOE unit enthalpy requirements. Then, operational current density (and, consequently SOE unit power density) is determined as the value that produces such overpotentials to equal thermoneutral voltage. In other words, operational voltage (represented by the SOE cells characteristic curve, Equation 10) and thermoneutral voltage (Equation 5) are equal.

Once current density is calculated and total current is known by assuming a reactant utilization coefficient and syngas Fischer Tropsch requirements, total SOE active area can be easily found.

Results

In this Section, results about the three systems are presented. It is important to remind the assumption that the design specification that determines components sizing is Fischer Tropsch liquid fuel productivity (Table 4) which is constant for all the evaluated configurations.

At first, for each block (SOE and FT) feeding streams flowrate and composition are shown, together with product streams flowrate and composition. The SOE performance section reports results concerning the electrolyzer, while the Fischer Tropsch performance section is relative to the liquid fuel synthesis. Then, efficiency calculations are performed, according to the definitions given at Equations 17 to 19 with regard to SOE and FT process respectively.

Finally, system performance and material consumption are calculated according to the definition given previously. All results concerning the system are reported and discussed in the Overall system evaluation section.

SOE performance

Table 5 reports cathode and anode feed streams and outlet streams of the SOE, calculated according to three layouts (A, B and C). After supplying the makeup streams, cathode feeding flowrates are the same for layouts A and B, while in layout C, in which reforming and shift take place inside the stack at 750°C, complete CO conversion to H_2

is not achieved and CO is still present amongst reactant species. Then, to obtain a H_2/CO ratio of 2.1 in the produced syngas, cathode inlet composition was modified with respect to layouts A and B, controlling the makeup flowrates of reactants after light gases recirculation from the syncrude separator block.

When performing reformate gases recirculation (layout B) and Fischer Tropsch light gases direct recovery (layout C), hydrogen content of recycled stream totally fulfils SOE requirements. In fact, hydrogen concentration achieved in both systems (7.3% and 7.8% respectively) satisfies the design requirements (Table 4).

Concerning anode inlet and outlet streams, flowrate and composition do not change with system layouts.

In all layouts SOE operates at thermoneutral voltage, calculated by the Fortran subroutine based on SOE characteristic V-j equation (10). Since negligible differences occur between the two experimental curves used for the linear regression of the V-j equation, it is reasonable to believe that Equation 10 is suitable for all layouts presented, despite slight variations in the cathode feeding composition.

In Figure 4, SOE stack polarization characteristic is plotted together with voltages related to the thermoneutral conditions of layouts A-B and layout C. The first voltage, referred as E_{tn1}, is calculated considering layout A-B enthalpy changes inside the stack. Then, the second one, E_{tn2}, is related to layout C enthalpy change. Thermoneutral conditions are calculated considering in the energy balance also the thermal energy necessary to preheat SOE reactants from 650°C to operational temperature and enthalpy variations of all reactions taking place in the electrolyzer.

INSERT TABLE 5

Hence, the model subroutine determines the operational point for each layout as the intersection of the polarization curve (POL, Figure 4) with the thermoneutral voltage. With a reactants utilization of 50%, in cases A and B, the stack worked at a power density of 0.716 W/cm^2 (E_{tn1}=1.39V). Conversely, in case C the stack working point is shifted to a higher value of power density, 0.735 W/cm^2 (E_{tn2}=1.40V).

INSERT FIGURE 4 HERE

Fischer Tropsch process performance

After water removal from SOE cathode outflow, dry syngas is fed to the Fischer Tropsch block: Table 6 shows Fischer Tropsch inlet stream composition. Taking this

input, the FT Aspen Plus® model, based on a discretized ASF distribution, gave the products spectrum shown in Figure 5.

INSERT FIGURE 5 HERE

A few carbon cuts were selected: methane (C1), propane and propene (C3), hexane and hexene (C6), octane and octane (C8), hexadecane and hexadecene (C16), waxes (C30). C6 are low-carbon number compounds which have to be further refined. Most of the production is shifted to middle and high carbon numbers (diesel). In this simulation, considering the application of a cobalt catalyst, the occurrence of oxygenates and polycyclic species was neglected. The model was tuned to get a daily liquid fuel production of 1 bbl, corresponding to a chemical storage potentiality of nearly 52 kW.

INSERT TABLE 6 HERE

Table 6, then, shows efficiency calculations performed according to the definition given above. The total energy efficiency of the system is 52.57% (Equation 18), while considering just the crude reaction as valuable product, gas-to-liquid efficiency is 40.95% (Equation 19). Power losses occurring when neglecting the gas fraction of the Fischer Tropsch products is recovered, at a system level, performing gas recirculation. Of course, this does not happen for the open loop design studied in layout A.

Overall system evaluation: layouts comparison

All results concerning the three system schemes presented in this work are displayed inTable 7. Model outcomes are expressed in terms of SOE stack features (thermoneutral voltage, active area, unit efficiency), net power required by the system (SOE power in, auxiliaries power in, net heat demand), power associated to crude production, exergy evaluation, efficiency indexes and material consumption coefficients.

Layout A

Layout A depicts system performance when neither material recirculation, nor heat recovery is performed. Such results were used mainly to assess single components performance. In particular, the FT block performance evaluated in layout A are equal to cases B and C, since FT feeding stream and operational conditions are imposed as design specifications. As a consequence, the auxiliary components (mainly the intercooled compressor) operating between the SOE and the FT process demand the same power consumption in all systems. Thus, considering SOE unit performance, results slightly differ just for cathode feeding composition change (in layout C the water

fraction is higher). This has an impact on the net electrical power required to reach thermoneutral conditions and on the thermal energy necessary to pre-heat reactants at SOE inlet temperature. Thus, SOE stack efficiency is lower in layout C than in layouts A and B.

INSERT TABLE 7 HERE

Layout B

The first scenario considers gases recirculation to the SOE cathode inlet. Feeding Fischer Tropsch light gases to an external reactor, performing separate reforming and shift conversion, hydrogen fraction substantially increases. Overall hydrogen gain is 56.2%, with regard to total hydrogen required at SOE cathode inlet. In detail, after the reforming stage, 27.2% of final hydrogen is recovered, while throughout the following shift conversion, the additional gain is 29%.

On one hand, this solution supplies entirely the system hydrogen demand (hydrogen net consumption is zero), but on the other hand, it entails some drawbacks: increased complexity and increased heat demand. Thus, the integrated system is equipped with two heat exchangers. The first is meant to produce superheated steam for the external reformer, assuming as hot source the Fischer Tropsch reactor. The latter is operated at 230°C and, since FT synthesis is exothermal, it needs cooling (waste heat is about 15.6 kW) to keep isothermal conditions. Figure 6 shows hot and cold curves for the heat recovery steam generator where reformer superheated steam is produced. However, superimposing a pinch-point temperature difference of 10°C, superheated steam exits the heat exchanger at 220°C and an additional heat source is necessary to superheat reforming steam from 220°C up to 700°C. Considering steam thermal capacity to satisfy a S/C=2, additional heat source power is 3.97 kW. Then, reformer reactor requires 4.93 kW to sustain the process at 700°C. This thermal power provides also the heat to raise light gases temperature from 25°C (Fischer Tropsch products separation tower conditions) to 700°C. Then, after the reformer stage, shift conversion takes place at 310°C; therefore, the second heat exchanger cools down reformate gases from 700°C to 310°C and waste heat (5.7 kW) is sufficient to vaporize the makeup water stream feeding the SOE cathode (Figure 6). Since the S/C ratio for the reformer is quite high, no more water is supplied to the shift converter.

Streams recirculation covers completely hydrogen requirements, but water and carbon dioxide net consumption are still positive and they call for a reintegration stream (with reference to base case layout A, water and carbon dioxide net consumption reductions are respectively 72% and 55%). Besides net consumption reduction, streams recirculation is useful also to increase system energy efficiency. In fact SOE cathode feed stream temperature is already high because recycled streams coming from the shift converter, that is operated at 310°C, are directly mixed with water and carbon dioxide makeup feed streams.

INSERT FIGURE 6 HERE

The overall energy efficiency for layout B, based on the definition given at Equation 20, is 56%. Exergetic efficiency, according to Equation 22, is 57.5% (Table 7).

Layout C

Performing internal reforming inside the SOE unit, the plant layout turns out to be less complex. Material consumption reduction is: 100% for hydrogen, 51% for carbon dioxide and 73% for water. Thus, cathode water and carbon monoxidemakeup stream flowrates were calculated based on the forecast stream composition after SOE internal reforming+shift equilibrium at 750°C is achieved. As a consequence of stack temperature (750°C), RWGS is expected to be favored and, for this, carbon monoxide is not totally shifted into hydrogen.

INSERT FIGURE 7 HERE

Recovered waste water is heated up to superheated steam, using the Fischer Tropsch reactor hot source, which is 15.6 kW. Heat exchanger hot and cold curves are depicted in Figure 7. Then, prior SOE inlet superheated steam is mixed to light gases coming from syncrude separation tower and makeup feed streams (water and carbon dioxide). Concerning the latter streams, makeup water needs an additional 4.85 kW heat source in order to complete phase transition to steam.

The overall energy efficiency of layout C, based on the definition given by Equation 20, is 57.2%, while, despite the highest p_{el}/p_{tot} ratio, exergetic efficiency, according to Equation 22, is 59.7% (Table 7). In comparison with previous results, it appears that layout C produces the best performance, together with a system complexity reduction. In addition to that, the change in cathode feeding composition together with a shift of the thermoneutral point leads to a minor extension of the SOE stack size (see active area

results, Table 7) , with an impact on the system costs. Despite the discussed advantages of layout C, this design introduces the risk of cell materials poisoning due to exposure to light gases; therefore, such issue could limit the applicability of layout C system design.

Conclusions

Our work aimed at showing a conceptual design of an electricity-to-liquid fuel system, made of a Solid Oxide Electrolyzer (SOE) stack working in co-electrolysis and a Fischer Tropsch reactor enhanced for middle-distillates production. In the outlook of distributed generation and energy storage, a basic assumption of this work was the Fischer Tropsch unit down-scaling, in order to couple the process with a RES-driven electrolyzer. Hence, crude fuel upgrading is to be done in a separate optimized plant, where primary Fischer Tropsch products can be easily conveyed and post processed.

A system-level model was built for three different system configurations: a basic open loop layout (A), a closed loop layout with reformate gases recirculation (B), a close loop layout with direct recirculation of Fischer Tropsch light gases (C). The SOE block was modelled according to experimental data; in the reference to base case (A) where inlet gas composition was H_2O:CO_2:H_2 58:34.5:7.5, at thermoneutral conditions SOE efficiency was estimated to be around 79% (LHV basis). Stack size, in order to supply enough syngas to feed a downstream 1 bbl/day Fischer Tropsch reactor, was expressed in terms of total active area required; hence the result is 10.43 m^2 with regard to the base case A. Then, taking into account all syncrude components, Fischer Tropsch energy efficiency was calculated to be 52.7% (LHV basis), while considering the crude fraction only, the efficiency is 40.95%. It is worth to recall that the efficiency of the synthesis is strongly dependent on the hypothesis about the catalyst which enhances CO conversion efficiency and selectivity on different carbon cuts.

The efficiency of the whole system was calculated for the three layouts, which differ from the point of view of waste streams recirculation and internal heat recovery management. Layouts B and C are closed-loop system design, aimed at increasing the performance in comparison with the base open-loop system design (layout A). Among them, the highest first law efficiency is achieved in layout C, where light gas fractions are recirculated directly to the SOE stack. Its energy efficiency is slightly higher than of layout B (57.2% versus 56%) and design complexity is much lower. However, it should

be reminded that degradation phenomena that could occur while supplying unreformed gas to the stack are not considered in this work. As far as material consumption is concerned, layout C achieves the following reductions: -73% water, -51% carbon dioxide and -100% hydrogen. From an exergetic point of view, layout C has a larger electrical consumption than layout B, since its thermoneutral condition is achieved at higher values of power density, namely 0.735 W/cm^2, instead of 0.716 W/cm^2. Layout C was found to have the best second law efficiency too. A follow-up of the study will consider a change in SOE operational temperature that may cause different results due to variation of thermal equilibrium and SOE efficiency.

Finally, keeping the liquid fuel daily productivity unchanged, the SOE stack size required is smaller for case C, with a further consequence on the economic viability of this solution.

Symbols and abbreviations

Abbreviations	**Description**	**Definition**
RES	Renewable energy sources	
SOE	Solid Oxide Electrolyzer	
FT	Fischer Tropsch	
WGS	Water gas shift reaction	
RWGS	Reverse water gas shift reaction	
Symbol	**Description**	**Definition**
i	Current	
E_{tn}	Thermoneutral voltage	$Etn = {\Delta H}/{zF}$
E_{rev}	Reversible voltage	$Erev = {\Delta G}/{zF}$
j	Current density	
A	Stack active area	$A = i \,/\, j$
z	Number of electrons needed to electrolyze one mole of reactants	
F	Faraday constant	96485 C/mol_e
Q_{react}	Reactants mole flowrate	
n	Number of carbon atoms	
α	Chain growth selectivity	
Wn	Mass fraction of the total of n-carbon atoms compounds	
$\left(\frac{O}{P}\right)_n$	Oleifins to paraffins ratio	
x_{COout}	CO molar fraction in the Fischer Tropsch syncrude	
x_{COin}	CO molar fraction in the Fischer Tropsch feeding stream	
LHV	Low heating value	
η	Theoretical electrolysis efficiency	
η_{ex}	System exergetic efficiency	

η_{FT}	Fischer Tropsch unit efficiency
η_{GTL}	Gas-to-liquid Fischer Tropsch unit efficiency
η_{SOE}	SOE stack efficiency
η_{tot}	Overall power-to-liquid efficiency
$(VI)_{soec}$	SOE stack electrical power requirements
W_{aux}	Auxiliary components power requirements
Q_{net}	Net thermal energy
S/C	Steam to carbon ratio

References

[1] Graves C, Ebbesen SD, Mogensen M, Lackner KS. Sustainable hydrocarbon fuels by recycling CO2 and H2O with renewable or nuclear energy. Renew Sustain Energy Rev 2011;15:1–23. doi:10.1016/j.rser.2010.07.014.

[2] Ferrero D, Lanzini A, Santarelli M, Leone P. A comparative assessment on hydrogen production from low- and high-temperature electrolysis. Int J Hydrogen Energy 2013;38:3523–36. doi:10.1016/j.ijhydene.2013.01.065.

[3] Gharibi H, Atikol U, Andrews J, Shabani B. Re-envisioning the role of hydrogen in a sustainable energy economy. Int J Hydrogen Energy 2012;37:1184–203.

[4] Kim S-D, Yu J-H, Seo D-W, Han I-S, Woo S-K. Hydrogen production performance of 3-cell flat-tubular solid oxide electrolysis stack. Int J Hydrogen Energy 2012;37:78–83. doi:10.1016/j.ijhydene.2011.09.079.

[5] Moçoteguy P, Brisse A. A review and comprehensive analysis of degradation mechanisms of solid oxide electrolysis cells. Int J Hydrogen Energy 2013:1–16. doi:10.1016/j.ijhydene.2013.09.045.

[6] Nguyen VN, Fang Q, Packbier U, Blum L. Long-term tests of a Jülich planar short stack with reversible solid oxide cells in both fuel cell and electrolysis modes. Int J Hydrogen Energy 2013;38:4281–90. doi:10.1016/j.ijhydene.2013.01.192.

[7] O'Brien JE, Stoots CM, Herring JS, Lessing PA, Hartvigsen JJ, Elangovan S. Performance Measurements of Solid-Oxide Electrolysis Cells for Hydrogen Production. J Fuel Cell Sci Technol 2005;2:156. doi:10.1115/1.1895946.

[8] Petipas F, Fu Q, Brisse A, Bouallou C. Transient operation of a solid oxide electrolysis cell. Int J Hydrogen Energy 2013;38:2957–64. doi:10.1016/j.ijhydene.2012.12.086.

[9] Udagawa J, Aguiar P, Brandon NP. Hydrogen production through steam electrolysis: Model-based steady state performance of a cathode-supported intermediate temperature solid oxide electrolysis cell. J Power Sources 2007;166:127–36. doi:10.1016/j.jpowsour.2006.12.081.

[10] Wang X, Yu B, Zhang W, Chen J, Luo X, Stephan K. Microstructural modification of the anode/electrolyte interface of SOEC for hydrogen production. Int J Hydrogen Energy 2012;37:12833–8. doi:10.1016/j.ijhydene.2012.05.093.

[11] Zhang H, Lin G, Chen J. Evaluation and calculation on the efficiency of a water electrolysis system for hydrogen production. Int J Hydrogen Energy 2010;35:10851–8. doi:10.1016/j.ijhydene.2010.07.088.

[12] Ebbesen SD, Mogensen M. Electrolysis of carbon dioxide in Solid Oxide Electrolysis Cells. J Power Sources 2009;193:349–58. doi:10.1016/j.jpowsour.2009.02.093.

[13] Petersen G, Viviani D, Magrini-Bair K, Kelley S, Moens L, Shepherd P, et al. Nongovernmental valorization of carbon dioxide. Sci Total Environ 2005;338:159–82. doi:10.1016/j.scitotenv.2004.06.025.

[14] Shi Y, Luo Y, Cai N, Qian J, Wang S, Li W, et al. Experimental characterization and modeling of the electrochemical reduction of CO2 in solid oxide electrolysis cells. Electrochim Acta 2013;88:644–53. doi:10.1016/j.electacta.2012.10.107.

[15] Stempien JP, Ding OL, Sun Q, Chan SH. Energy and exergy analysis of Solid Oxide Electrolyser Cell (SOEC) working as a CO2 mitigation device. Int J Hydrogen Energy 2012;37:14518–27. doi:10.1016/j.ijhydene.2012.07.065.

[16] Zhan Z, Zhao L. Electrochemical reduction of CO2 in solid oxide electrolysis cells. J Power Sources 2010;195:7250–4. doi:10.1016/j.jpowsour.2010.05.037.

[17] Bierschenk DM, Wilson JR, Barnett S a. High efficiency electrical energy storage using a methane–oxygen solid oxide cell. Energy Environ Sci 2011;4:944. doi:10.1039/c0ee00457j.

[18] Ebbesen SD, Graves C, Mogensen M. Production of Synthetic Fuels by Co-Electrolysis of Steam and Carbon Dioxide. Int J Green Energy 2009;6:646–60. doi:10.1080/15435070903372577.

[19] Ebbesen SD, Høgh J, Nielsen KA, Nielsen JU, Mogensen M. Durable SOC stacks for production of hydrogen and synthesis gas by high temperature electrolysis. Int J Hydrogen Energy 2011;36:7363–73. doi:10.1016/j.ijhydene.2011.03.130.

[20] Graves C, Ebbesen SD, Mogensen M. Co-electrolysis of CO2 and H2O in solid oxide cells: Performance and durability. Solid State Ionics 2011;192:398–403. doi:10.1016/j.ssi.2010.06.014.

[21] Li W, Wang H, Shi Y, Cai N. Performance and methane production characteristics of H2O–CO2 co-electrolysis in solid oxide electrolysis cells. Int J Hydrogen Energy 2013;38:11104–9. doi:10.1016/j.ijhydene.2013.01.008.

[22] Stoots C, O'Brien J, Hartvigsen J. Results of recent high temperature coelectrolysis studies at the Idaho National Laboratory. Int J Hydrogen Energy 2009;34:4208–15. doi:10.1016/j.ijhydene.2008.08.029.

[23] Sunfire. Sunfire power-to-liquid n.d. http://www.sunfire.de/en/produkte/fuel/power-to-liquids.

[24] Perego C, Bortolo R, Zennaro R. Gas to liquids technologies for natural gas reserves valorization: The Eni experience. Catal Today 2009;142:9–16. doi:10.1016/j.cattod.2009.01.006.

[25] Wilhelm D., Simbeck D., Karp a. ., Dickenson R. Syngas production for gas-to-liquids applications: technologies, issues and outlook. Fuel Process Technol 2001;71:139–48. doi:10.1016/S0378-3820(01)00140-0.

[26] Hamelinck C, Faaij a, Denuil H, Boerrigter H. Production of FT transportation fuels from biomass; technical options, process analysis and optimisation, and development potential. Energy 2004;29:1743–71. doi:10.1016/j.energy.2004.01.002.

[27] Hu J, Yu F, Lu Y. Application of Fischer–Tropsch Synthesis in Biomass to Liquid Conversion. Catalysts 2012;2:303–26. doi:10.3390/catal2020303.

[28] Zhu XG, Long SP, Ort DR. What is the maximum efficiency with which photosynthesis can convert solar energy into biomass? Curr Opin Biotechnol 2008;19:153–9. doi:10.1016/j.copbio.2008.02.004.

[29] Pro BH, Hammerschlag R, Mazza P. Energy and land use impacts of sustainable transportation scenarios. J Clean Prod 2005;13:1309–19. doi:10.1016/j.jclepro.2005.05.005.

[30] O'Brien JE, McKellar MG, Stoots CM, Herring JS, Hawkes GL. Parametric study of large-scale production of syngas via high-temperature co-electrolysis. Int J Hydrogen Energy 2009;34:4216–26. doi:10.1016/j.ijhydene.2008.12.021.

[31] O'Brien JE, McKellar MG, Harvego E a., Stoots CM. High-temperature electrolysis for large-scale hydrogen and syngas production from nuclear energy – summary of system simulation and economic analyses. Int J Hydrogen Energy 2010;35:4808–19. doi:10.1016/j.ijhydene.2009.09.009.

[32] Sun X, Chen M, Jensen SH, Ebbesen SD, Graves C, Mogensen M. Thermodynamic analysis of synthetic hydrocarbon fuel production in pressurized solid oxide electrolysis cells. Int J Hydrogen Energy 2012;37:17101–10. doi:10.1016/j.ijhydene.2012.08.125.

[33] Fouih Y El, Bouallou C. Recycling of Carbon Dioxide to Produce Ethanol. Energy Procedia 2013;37:6679–86. doi:10.1016/j.egypro.2013.06.600.

[34] Redissi Y, Bouallou C. Valorization of Carbon Dioxide by Co-Electrolysis of CO2/H2O at High Temperature for Syngas Production. Energy Procedia 2013;37:6667–78. doi:10.1016/j.egypro.2013.06.599.

[35] Becker WL, Braun RJ, Penev M, Melaina M. Production of Fischer–Tropsch liquid fuels from high temperature solid oxide co-electrolysis units. Energy 2012;47:99–115. doi:10.1016/j.energy.2012.08.047.

[36] Shell GtL n.d. http://www.shell.com/global/future-energy/natural-gas/gtl/story/accessible-version.html.

[37] PetroSA n.d. http://www.petrosa.co.za/.

[38] Sasol n.d. http://www.sasol.com/.

[39] Rentech n.d. http://www.rentechinc.com/.

[40] Hargreaves N. Smaller scale GTL – effective gas monetisation. 2014.

[41] Steynberg AP, Dry ME. Fischer-Tropsch technology. Studies in. Elsevier; 2004.

[42] Yates I, Satterfield C. Intrinsic kinetics of the Fischer-Tropsch synthesis on a cobalt catalyst. Energy Fuels 1991;5:168–73.

[43] Penchini D, Cinti G, Discepoli G, Desideri U. Theoretical study and performance evaluation of hydrogen production by 200 W solid oxide electrolyzer stack. Int J Hydrogen Energy 2014;39:9457–66. doi:10.1016/j.ijhydene.2014.04.052.

[44] Di Michele A. Sonochemical synthesis of metal nanoclusters and their use in the Fischer-Tropsch process. Università degli Studi di Perugia, 2007.

[45] Tavakoli A, Sohrabi M, Kargari A. Application of Anderson–Schulz–Flory (ASF) equation in the product distribution of slurry phase FT synthesis with nanosized iron catalysts. Chem Eng J 2008;136:358–63. doi:10.1016/j.cej.2007.04.017.

[46] Shi B, Davis BH. Fischer–Tropsch synthesis: The paraffin to olefin ratio as a function of carbon number. Catal Today 2005;106:129–31. doi:10.1016/j.cattod.2005.07.159.

Table 1 Jülich short-stack features

Anode substrate	Ni/8YSZ cermet 1500 □m
Anode functional layer	Ni/8YSZ cermet 7–10 □m
Electrolyte	8YSZ 8–10 □m
Cathode functional layer	LSM/8YSZ 10–15 □m
Cathode current collector	LSM 60–70 □m
Stack design	F-design
Interconnect/cell frame	Crofer22APU
Anode contact layer	Ni-mesh
Cathode contact layer	Perovskite type oxide (LCC10)
Sealing	Glass-ceramic (87YSZ20)
Number of cells	4
Size of cells	100 × 100 mm²
Active area per cell	80 cm²

Table 2 SOE experimental campaign: two tests were carried out varying cathode feeding composition.

Electrode feeding composition		**Test 30-60-10**		**Test 40-50-10**	
CATHODE	CO_2 *[mol/h]*	2.56	30%	3.41	40%
	H_2O *[mol/h]*	5.12	60%	4.26	50%
	H_2 *[moll/h]*	0.85	10%	0.85	10%
ANODE	Air *[mol/h]*	8.92	100%	8.92	100%

Table 3 Fischer Tropsch products: for every carbon cut considered, model compounds are selected. Then, polymerization reactions for selected model compounds are shown.

n range	**Cut**	**Model n**	**Model molecules**	**Reaction**
n=1	Light gases 1	1	Methane	$CO + 3\,H_2 \rightarrow CH_4 + \ H_2O$
2≤n≤4	Light gases 2	3	Propane	$3CO + 7\,H_2 \rightarrow C_3H_8 + \ 3\,H_2O$
			Propene	$3\ CO + 6\,H_2 \rightarrow C_3H_6 + \ 3\,H_2O$
5≤n≤6	C5-C6	6	Exane	$6CO + 13\,H_2 \rightarrow C_6H_{14} + \ 6\,H_2O$
			Exene	$6\ CO + 12\,H_2 \rightarrow C_6H_{12} + \ 6\,H_2O$
7≤n≤10	Gasoline	8	Octane	$8\ CO + 17\,H_2 \rightarrow C_8H_{18} + \ 8\,H_2O$
			Octene	$8\ CO + 16\,H_2 \rightarrow C_8H_{16} + \ 8\,H_2O$
11≤n≤19	Middle distillates (Diesel)	16	Cetane	$16\ CO + 33\,H_2 \rightarrow C_{16}H_{34} + \ 16\,H_2O$
			Cetene	$16\ CO + 32\,H_2 \rightarrow C_{16}H_{32} + \ 16\,H_2O$
n≥20	Waxes	30	Paraffin wax (C30)	$30\ CO + 61\,H_2 \rightarrow C_{30}H_{62} + \ 30\,H_2O$

Table 4 Model design specification summary

Model section	Design specification	Set point	Layout
SOE	Anode feeding inlet temperature	120°C	A,B,C
SOE	SOE operational temperature and pressure	750°C, 1 bar	A,B,C
SOE	SOE operative point	Thermoneutral	A,B,C
SOE	Cathode feeding H_2+CO concentration	7-8%	A,B,C
SOE	Anode outflow O_2 concentration	50%	A,B,C
SOE	Reactant utilization	50%	A,B,C
SOE	Cathode outflow H_2/CO ratio	2.10	A,B,C
FT	Synthesis temperature and pressure	230°C, 20 bar	A,B,C
FT	Chain growth probability	0.94	A,B,C
FT	CO conversion efficiency	0.87	A,B,C
FT	Crude synthesis productivity	1 bbl/day	A,B,C
External Reformer	Steam-to-Carbon ratio	2	B
External Reformer	Reforming temperature and pressure	700°C, 1 bar	B
External Shift converter	WGS temperature and pressure	310°C, 1 bar	B
Heat exchangers	Temperature difference at pinch point	10°C	B,C

Table 5 SOE model results. Cathode outflow composition is the same for layout A, B and C. Unit performances calculated in the table are relative to SOE stack operating without feeding recycled and heat recovery (layout A). *7.8% is the overall molar fraction given by the sum of hydrogen and carbon monoxide.

	Layouts A and B		**Layout C**		**Layouts A, B, C**	
	Cathode feed *[mol/h]*	Mole frac *[%]*	Cathode feed *[mol/h]*	Mole frac *[%]*	Cathode out *[mol/h]*	Mole frac *[%]*
H_2O	1259	58.2%	1303	60.2%	631	29.2%
CO_2	745	34.5%	691	32.0%	372	17.2%
H_2	158	7.3%	117	7.8%*	783	36:2%
CO	-	-	51		374	17.3%
CH_4	-	-	-	-	1.33	0.1%
Total	2162	100%	2162	100%	2162	100%
	Anode feed *[mol/h]*	Mole frac *[%]*	Anode feed *[mol/h]*	Mole frac *[%]*	Anode out *[mol/h]*	Mole frac *[%]*
O_2	*180*	*21%*	*180*	*21%*	681	*50%*
N_2	*681*	*79%*	*681*	*79%*	1362	*50%*
Total	861	100%	861	100%	1430	100%

Table 6 Fischer Tropsch input streams and products. Syncrude refers to the whole products stream going out of the Fischer Tropsch reactor, while Crude relates to Fischer Tropsch deprived of light gases. Power and efficiency calculations are based on species LHV.

FT inputs (layouts A, B, C)				
	Feed flow rate *[mol/h]*		Mole fraction *[%]*	
H_2	783		51.2%	
H_2O	0		0%	
CO	374		24.4%	
CO_2	372		24.3%	
CH_4	1.33		0.1%	
Total	1532		100%	
H2/CO	2.10			
SYNCRUDE				
	Components mole flow *[mol/h]*	Components mole fraction *[%]*	Power output *[kW]*	Power allocation *[%]*
H_2	69.07	8.16%	4.55	6.83%
H_2O	345.37	40.78%	0.00	0.00%
CO	30.29	3.58%	5.55	8.33%
CO_2	372.12	43.94%	0.00	0.00%
CH_4	3.39	0.40%	0.76	1.14%
C_3H_6	2.29	0.27%	1.22	1.83%
C_3H_8	3.21	0.38%	1.83	2.75%
C_6H_{12}	0.51	0.06%	0.55	0.83%
C_6H_{14}	2.69	0.32%	2.96	4.44%
C_8H_{16}	0.47	0.06%	0.57	0.86%
C_8H_{18}	4.86	0.57%	5.84	8.76%
$C_{16}H_{32}$	0.06	0.01%	0.17	0.25%

$C_{16}H_{34}$	7.98	0.94%	20.89	31.36%
$WAXC_{30}$	4.48	0.53%	21.74	32.63%
Energy efficiency				
Power in	*[kW]*	126.4		
Power out	*[kW]*	66.28		
Efficiency	*[%]*	52.57%		

CRUDE		
	Crude production *[bbl/day]*	Power allocation *[kW]*
C_6	0.06	2.67
Gasoline	0.15	6.17
Diesel	0.43	21.06
$WAXC_{30}$	0.36	21.74
Total	1.00	51.63
Gas-to-liquid		
Power in	*[kW]*	126.4
Power out	*[kW]*	52
Efficiency	*[%]*	40.95%

Table 7 System performance in cases A (basic SOE and Fischer Tropsch integration), B (SOE and Fischer Tropsch integration, with external steam reforming and cathode feed recirculation), C (SOE and Fischer Tropsch integration, with internal steam reforming and cathode feed recirculation).

		Layout A	**Layout B**	**Layout C**
Power in	*[kW]*	87.92	77.63	79.70
Auxiliaries Power in	*[kW]*	5.7	5.7	5.7
Q net,system	*[kW]*	17.54	8.90	4.86
Power out (Crude)	*[kW]*	51.63	51.63	51.63
E_{tn}	*[V]*	1.39	1.39	1.40
A	*[m^2]*	10.43	10.43	10.21
η_{SOE}	*[%]*	79%	79%	78%
η_{GTL}	*[%]*	40.95%	40.95%	40.95%
η_{tot}	*[%]*	46.4%	56.0%	57.2%
W in	*[kW]*	98.07	89.54	86.45
W out	*[kW]*	51.63	51.63	51.63
η_{ex}	*[%]*	52.6%	57.7%	59.7%
$\frac{p_{el}}{p_{tot}}$	*[%]*	69.7%	88.0%	90.1%
H_2O consumption	*[ton/MJ]*	121944	33707 (-72%)	33701 (-73%)
H_2 consumption	*[ton/MJ]*	1694	0 (-100%)	0 (-100%)
CO_2 consumption	*[ton/MJ]*	176397	79844 (-55%)	79795 (-51%)

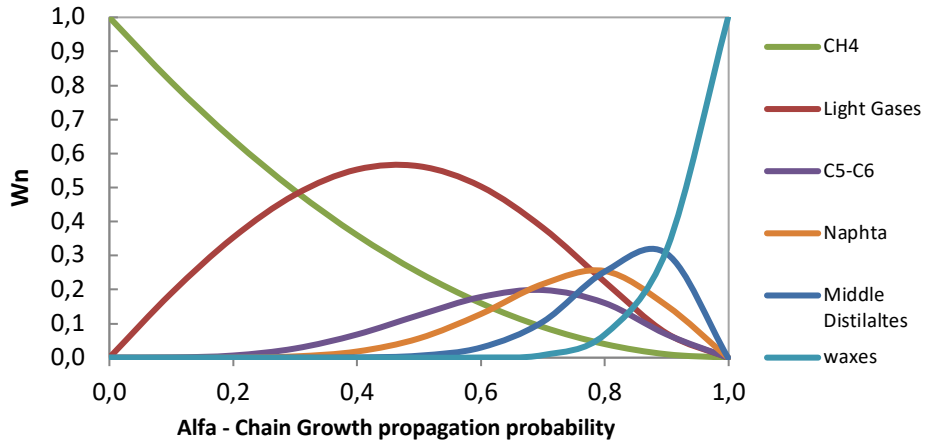

Figure 1 Fischer Tropsch products spectrum: mass fraction of several carbon cuts versus catalyst Chain Growth probability.

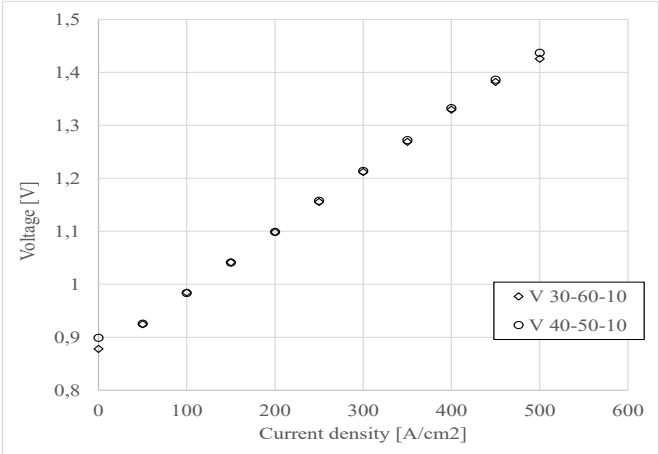

Figure 2 SOE experimental results: polarization curves (average on four cells) obtained on Table 2 cathode feeding compositions.

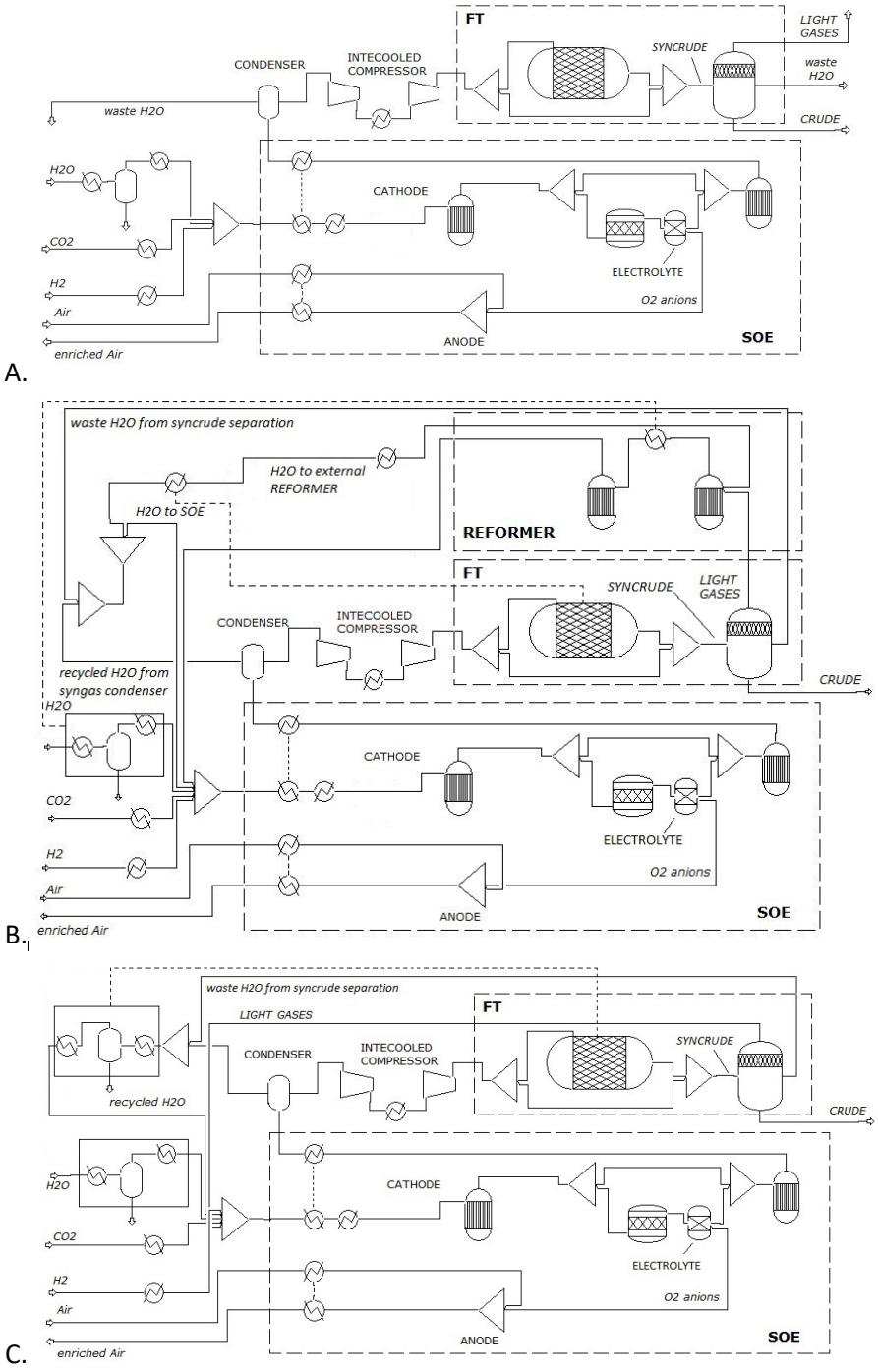

Figure 3 System layouts: basic integration of SOE with FT (A), recirculation of reformate Fischer Tropsch lighter gases to SOE inlet (B), recirculation of unreformed Fischer Tropsch lighter gases to SOE inlet (C)

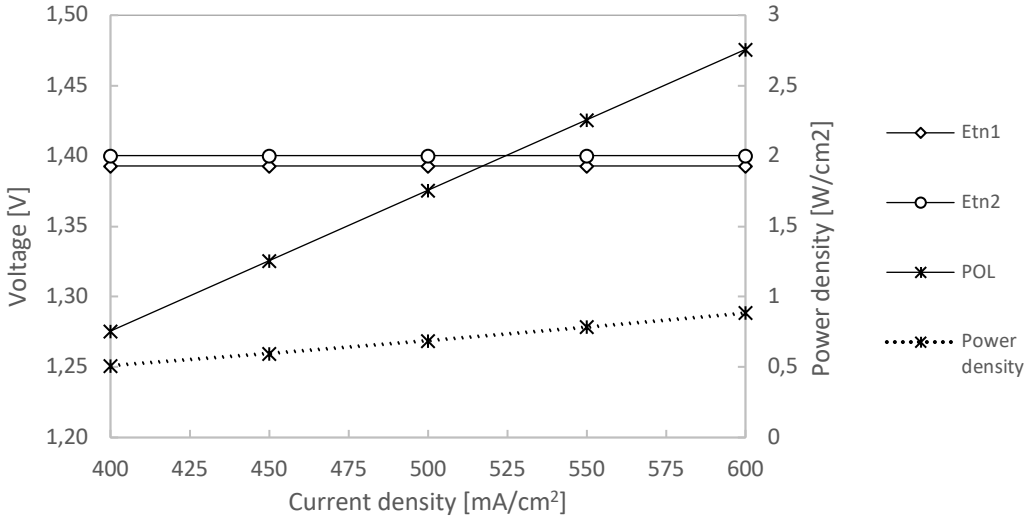

Figure 4 SOE operational point definition: SOE polarization curve based on experimental data regression is plotted together with thermoneutral voltages calculations derived from model enthalpy balance. E_{tn1} is thermoneutral voltage for system layouts A and B, while E_{tn2} refers to layout C

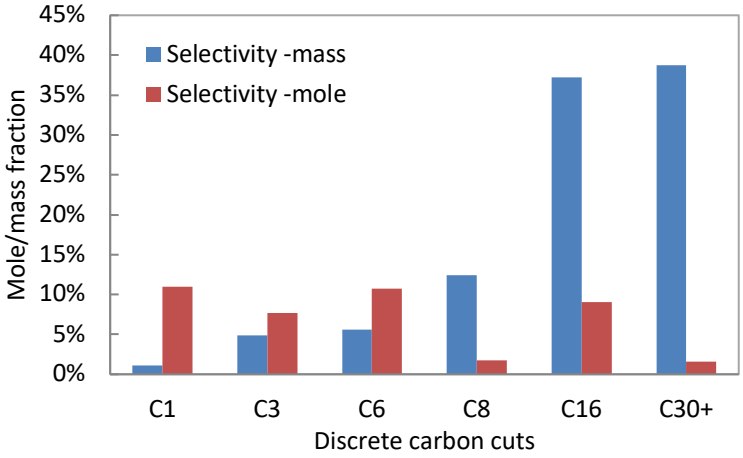

Figure 5 Aspen Fischer Tropsch model results: products mole and mass fractions. Products spectrum reflects superimposed assumptions about catalyst selectivity.

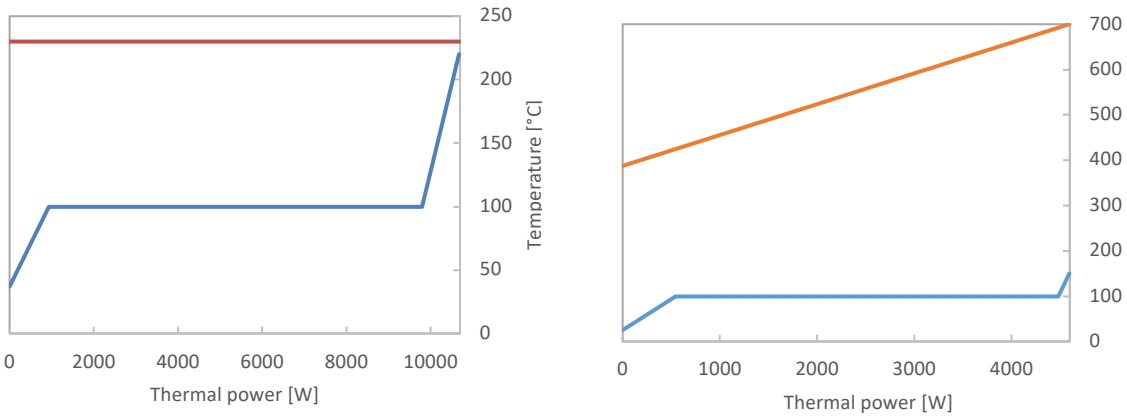

Figure 6 Layout B heat exchangers diagrams: left) Fischer Tropsch reactor cooling thermal balance: heat sink is H2O recycled to the reformer; right) cold stream is reintegration water, hot stream is reformed gas

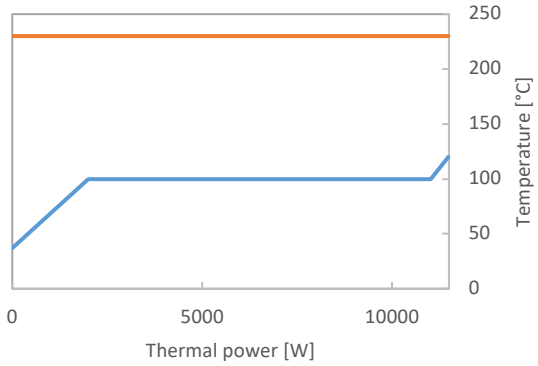

Figure 7 Layout C heat exchanger diagrams: Fischer Tropsch heat is used to evaporate water and to achieve superheating.